IOSR Journal of Applied Physics (IOSR-JAP)
e-ISSN: 2278-4861.Volume 11, Issue 4 Ser. I (Jul. – Aug. 2019), PP 76-79
www.iosrjournals.org

Magnetic Properties, Phase Transformation and Structural Studies on Amorphous $Fe_{78}Ce_2B_{20}$ Alloy

B. Bhanu Prasad,
Department of Sciences & Humanities, M.V.S.R. Engineering College, Nadergul, Hyderabad – 501 510.
Corresponding Author: B. Bhanu Prasad

Abstract: *Magnetic properties, amorphous to crystalline transformation and structure of amorphous $Fe_{78}Ce_2B_{20}$ alloy have been studied to understand its thermal stability. Vibration Sample Magnetometer (VSM), Four Probe Electrical Resistivity (FPER) and X-ray Diffraction (XRD) are used in this study. FPER is used in the temperature range 300 K - 900 K. The sample showed single-step crystallization. The resistivity of amorphous $Fe_{78}Ce_2B_{20}$ ar room temperature (ρ_{RT}) is found to be 162.44 $\mu\Omega$-cm. The temperature coefficient of resistivity (TCR) and Debye temperature (θ_D) of the sample are found to be 5.88 X $10^{-4}K^{-1}$ and 390.74 K, respectively. From XRD showed the presence of α-Fe, orthorhombic FeB Phase , Tetragonal Fe_2B Phase and Tetragonal Fe_3B Phases are in the crystallized sample.*

Keywords*: differential scanning calorimetry, activation energy, crystallization behavior, thermal stability, crystallization temperature*

Date of Submission: 10-07-2019 Date of acceptance: 25-07-2019

I. Introduction

Rare Earth (RE) containing iron rich amorphous ferromagnetic alloys , obtained in amorphous state by Melt-Spinning method have been considered due to their enhanced magnetic, electrical and mechanical properties [1,2]. Thus, the use of rare earth in Fe-B group alloys has increased significantly in a number of industrial fields over the past few decades. The demand of these magnets is increasing because these magnets are indispensable for high performance motors in electric vehicles [3-7]. These magnets need to possess sufficient thermal stability for use in such motors in high temperature environments. The thermal stability of these amorphous alloys is a subject of considerable interest, since the properties of these engineering materials may be significantly changed by the onset of crystallization and crystallization is associated with nucleation and growth process.

In this paper, I discussed the magnetic properties, phase transformation and structure of amorphous $Fe_{78}Ce_2B_{20}$.

II. Experimental

Amorphous $Fe_{78}Ce_2B_{20}$ alloy is procured commercially which was prepared by the melt-spinning technique. The ribbons were about 1 mm wide and 30 µm thick. The amorphous state of the ribbons was initially confirmed by taking XRD for the fresh samples. Magnetic properties of the sample are measured at room temperature using VSM. FPER is used to measure voltage developed between the voltage contacts at constant current in the temperature range 300 K - 900 K. XRD of the crystallized sample is also recorded at room temperature.

III. Results And Discussion

The rare earth- transition metal (RE-TM) interaction proceeds via an indirect mechanism. It was proposed that 5d electrons are involved as the intermediary. There is intra-atomic exchange coupling between 4f and 5d electrons, and an interatomic interaction between 5d and 3d electrons. The 4f-5d interaction is ferromagnetic, but the 5d-3d interaction is antiferromagnetic . When the 5d band is less than half full and the 3d band is more than half full, the ferromagnetic transition metal spin couples anti parallel to the rare earth spin. Hence, the magnetization of rare-earth and transition metal sub lattices couple parallel for the light rare-earth like Ce (J=L-S) and antiparralel for Gd and the other heavy rare-earths (J=L+S). The average magnetic moment μ_M per magnetic atom can be derived from the formula

$$\mu_M = (\sigma.M)/(N.\mu_B) \quad \text{…………………(1)}$$

where **σ** *is magnetization,* ***M*** is the molecular weight of the $Fe_{78}Ce_2B_{20}$ alloy, *N* is Avogadro's number and μ_B is the Bohr magneton. The alloy moment (μ_a) can be written as

$$\mu_a= [(80-x)\mu_{Fe} + x\mu_{Ce}]/100 \quad \text{……………….(2)}$$

where μ_{Fe} and μ_{Ce} denote the magnetic moments of Fe and Ce respectively [8] . Taking μ_{Ce} as $2.14\mu_B$ [9], Fe magnetic moment is calculated. It is known that with the addition of Ce metal, the Fe ion magnetic moment decreases due to hybridization of the 5d and 3d orbitals.

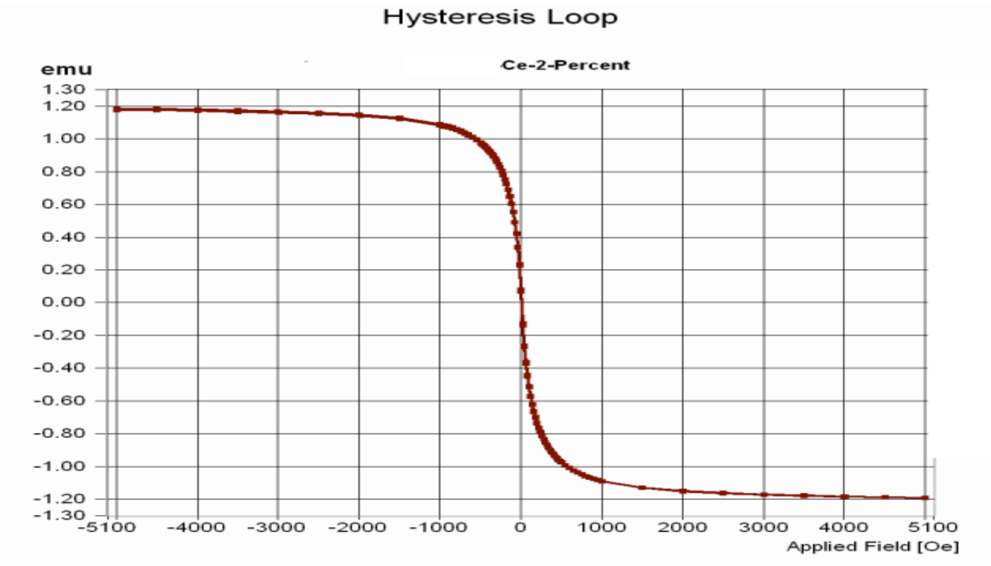

Figure 1 The Hysteresis curve of amorphous $Fe_{78}Ce_2B_{20}$ alloy

Table 1: Sample, Coercive field (Oe), Saturation Magnetization per gram, M_s/gram (emu), Residual Magnetization, M_r (emu), Magnetic Moment of RE (μ_B) and Magnetic Moment of Fe(μ_B)

Before heating (Fresh $Fe_{78}Ce_2B_{20}$ sample)

Sample	H_c (Oe)	M_s/gram (emu)	M_r (emu) at H=0	μ for free Ce ion (μ_B*)	μ for Fe ion (μ_B)
$Fe_{76}Ce_2B_{20}$	0.5	126.32	$2.651E^{-3}$	2.14	1.71

***Taken from Literature**

Table 2: Sample, Coercive field (Oe), Saturation Magnetization per gram, M_s/gram (emu), Residual Magnetization, M_r (emu), Magnetic Moment of Ce (μ_B) and Magnetic Moment of Fe(μ_B)

After heating (Crystallized $Fe_{78}Ce_2B_{20}$ sample)

Sample	H_C (Oe)	Ms (emu)	Ms/gram (emu)	Mr (emu) M at H=0	μ for Ce ion (μ_B)	μ for Fe ion (μ_B)	μ for free Ce ion (μ_B*)
$Fe_{76}Ce_2B_{20}$	106.35	4.691^{E-1}	167.53	7.473^{E-2}	5.4875	2.28	2.14

***Taken from Literature**

Room temperature hysteresis loop of the as-quenched sample $Fe_{78}Ce_2B_{20}$ is shown in Fig. 1. Thus, Table 1 gives the Coercive field (Oe), Saturation Magnetization per gram, M_s/gram (emu), Residual Magnetization, M_r (emu), Magnetic Moment of RE (μ_B) and Magnetic Moment of Fe(μ_B) of amorphous (as quenched) $Fe_{78}Ce_2B_{20}$ alloy. The coercive field of amorphous $Fe_{76}Ce_2B_{20}$ is 0.5 Oe. Table 2 gives the Coercive field (Oe), Saturation Magnetization per gram, M_s/gram (emu), Residual Magnetization, M_r (emu), Magnetic Moment of RE (μ_B) and Magnetic Moment of Fe(μ_B) of crystallized $Fe_{78}Ce_2B_{20}$ alloy. From the two Tables, it is clear that the coercive field, saturation magnetization and magnetic moment of iron increase when we move to crystallized samples.

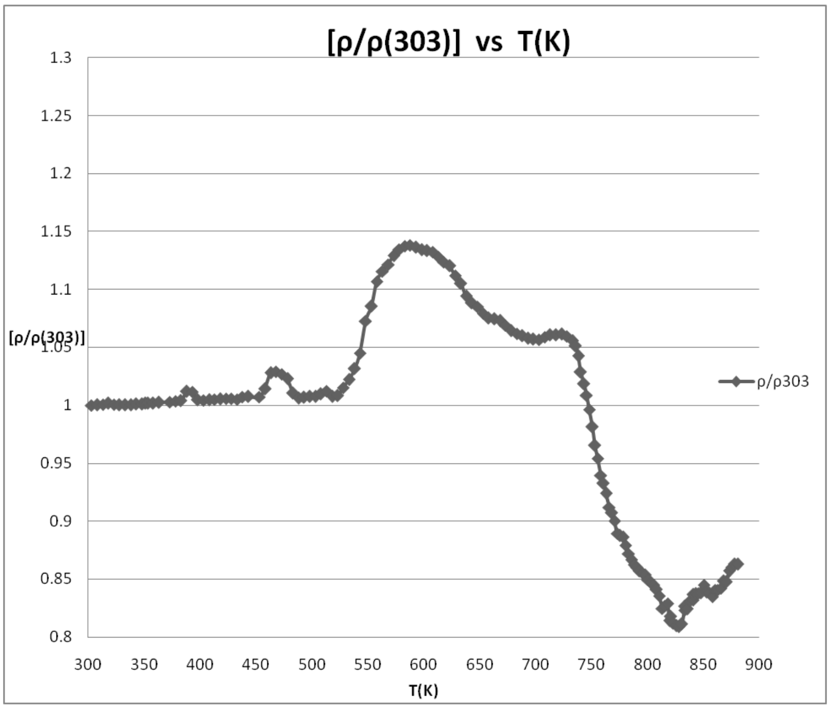

Figure 2: Resistivity Ratio, $\rho/\rho_{(303)}$ versus Temperature (T) of amorphous $Fe_{78}Ce_2B_{20}$ alloy

Figure 2 shows the variation of resistivity ratio with temperature of amorphous $Fe_{78}Ce_2B_{20}$ alloy. As in Fig. 2, the curve shows a small broad peak around 388 K, slightly bigger broad peak at 468 K and a broad peak (bump) around 583 K. The amorphous sample shows onset of crystallization at 723 K and the crystallization is complete at 830.5 K. Thus a drop in the resistivity ratio is observed between 723 K and 830.5 K which shows amorphous to crystalline transformation in the sample. This reveals that a single step crystallization occurs in the sample. The room temperature resistivity, temperature coefficient of resistivity (TCR) and Debye temperature (θ_D) of amorphous $Fe_{78}Ce_2B_{20}$ alloy are found to be 162.44 μΩ-cm, 5.88 X $10^{-4}K^{-1}$ and 390.74 K, respectively.

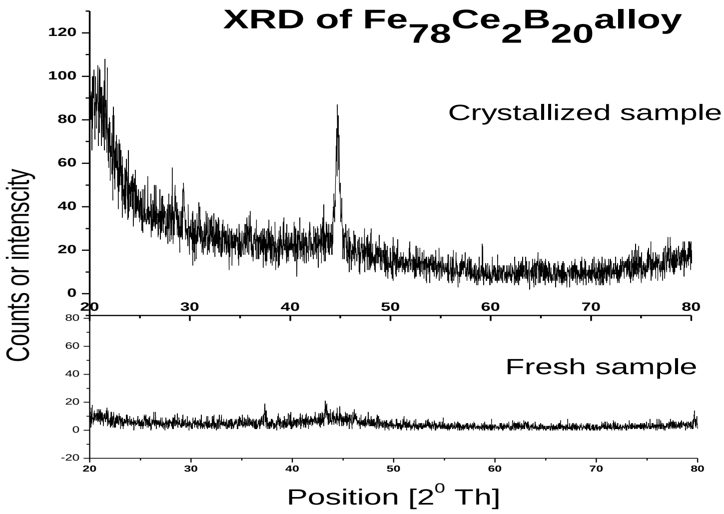

Figure 3 XRD pattern of amorphous and crystallized $Fe_{78}Ce_2B_{20}$ alloy recorded at room temperature.

Figure 3 shows the XRD patterns of $Fe_{78}Ce_2B_{20}$ (amorphous and crystallized), recorded at room temperature. XRD pattern of as quenched or fresh sample shows amorphous nature as Boron is known to facilitate the formation of amorphous structure. XRD pattern of the crystallized sample shows a sharp peak around $2\theta=44^0$ (Fig.3), indicating the presence of cubic α-Fe phase in the sample as mentioned in Table 3. Thus, Table 3 also shows the sample composition, phases in the crystallized sample, diffraction data, lattice parameters, Cell Volume and Crystallite size. From our study, when 2% of Ce is added to Fe-B alloy, the crystallized sample consists of mostly α-Fe phase. Table 3 also indicates that in addition to α-Fe, orthorhombic FeB Phase , Tetragonal Fe_2B Phase and Tetragonal Fe_3B Phase are also present in the crystallized sample.

Table 3: Sample composition, phases in the crystallized sample, diffraction data, lattice parameters, Cell Volume and Crystallite size.

Element	Phases obtained	2003 JCPDS Inter National Centre for diffraction data	Lattice parameters(A^0)			Cell Volume(A^0)	Crystallite size
		Card No.	aA^0	b A^0	c A^0		
Fe_{78} Ce_2B_{20}	Cubic α-Fe	65.4899	2.866			23.5411	$4.235\ x10^{-10}$m
	A small amount of orthorhombic FeB Phase	76-0092	4.053	5.495	2.946	65.611	
	A small amount of Tetragonal Fe_2B Phase	39-1314	5.1317		8.5325	224.69	
	A small amount of Tetragonal Fe_3B Phase	33.0644	8.63		4.29	319.5	

IV. Conclusions

Amorphous $Fe_{78}Ce_2B_{20}$ alloy showed a perfect Hysteresis curve confirming that it is a ferromagnet. The coercive field, saturation magnetization and magnetic moment of iron increase when we move from amorphous to crystallized samples. The room temperature resistivity, temperature coefficient of resistivity (TCR) and the Debye temperature (θ_D) of amorphous $Fe_{78}Ce_2B_{20}$ alloy are 162.44 μΩ-cm, $5.88\ X\ 10^{-4}K^{-1}$ and 390.74 K, respectively. From XRD studies, it is confirmed that α-Fe phase in the amorphous matrix of the sample. In addition to α-Fe, orthorhombic FeB Phase , Tetragonal Fe_2B Phase and Tetragonal Fe_3B Phases are present in the crystallized sample.

Acknowledgements

The author B. Bhanu Prasad acknowledge the encouragement given by the Management, the Principal, HOD of Sciences & Humanities and the staff of M.V.S.R. Engineering College, Nadergul, Hyderabad.

References

[1]. R. Skomski, J. Appl. Phys., **76** (1994) 7059
[2]. R. Fischer, T. Schrefl, H. Kronmuller and J. Fidler, J. Magn. Magn. Mat., **150** (1995) 329
[3]. C.B. Carter and M.G. Norton, (2007), Ceramic Materials Science and Engineering, Springer, ISBN-10: 0387462708, New York, USA.
[4]. E.B. Araújo and E. Idalgo, *Journal of Thermal Analysis and Calorimetry*, **95** (2009) 37
[5]. E.B. Araujo, E. Idalgo, A.P.A. Moraes, A.G. Souza Filho and Mendes Filho, J., *Mat. Res. Bull.*, **44** (2009) 1596
[6]. Zhao-hua Cheng, Bao-gen Shen, Ming-xi Mao, Ji-jun Sun, Yi-de Zhang, and Fa-shen Li, Phys. Rev. B **52** (1995) 9427
[7]. O. Crisana, J.M. Le Bretonc, F. Machizaudd, Y. Labayeb and G. Filotia, J. Magn. and Magn. Mater., **242–245** (2002) 1297
[8]. R. Krishnan, H. Lassri, J. Teillet, J. Magn. Magn. Mat. **98** (1991) 155
[9]. J.M.D. Coey, Rare – Earth Iron Permanent Magnets, Oxford Science Publications.

IOSR Journal of Applied Physics (IOSR-JAP) is UGC approved Journal with Sl. No. 5010, Journal no. 49054.

B. Bhanu Prasad. " Magnetic Properties, Phase Transformation and Structural Studies on Amorphous Fe78Ce2B20 Alloy.” IOSR Journal of Applied Physics (IOSR-JAP) , vol. 11, no. 4, 2019, pp. 76-79.